

# Solvothermal synthesis and characterization of anatase TiO<sub>2</sub> nanocrystals with ultrahigh surface area

Rajeev K. Wahi, Yunping Liu<sup>\*</sup>, Joshua C. Falkner, Vicki L. Colvin<sup>\*</sup>

*Chemistry Department, MS-60, Center for Biological and Environmental Nanotechnology, Rice University, Houston, TX 77005-1892, USA*

Received 9 December 2005; accepted 5 July 2006

Available online 11 July 2006

## Abstract

Phase-pure, ultrafine nanocrystalline anatase with high specific surface area (up to 250 m<sup>2</sup> g<sup>-1</sup>) was obtained upon injection of a titanium alkoxide precursor into ethanol with designed volume of water under mild solvothermal conditions (<200 °C, 2 h). Primary particle sizes were tuned by adjusting various reaction parameters, with the smallest grain sizes occurring at low temperatures (140–150 °C), low initial alkoxide concentrations, and intermediate hydrolysis ratios ( $r \equiv [\text{H}_2\text{O}]/[\text{Ti}(\text{OR})_4] = 5\text{--}10$ ). Additionally, variations in the reaction temperature result in changes in particle morphology and distribution, with high-temperature samples exhibiting bimodal distributions of small spherical and larger cubic particles that suggest grain growth via Ostwald ripening. A crystalline product with high thermal stability and specific surface area up to 5 times that of commercial nano-titania can be obtained at a relatively low temperature of 150 °C. The physical properties of the titania samples obtained in this study suggest they might be well suited for catalytic applications.

© 2006 Elsevier Inc. All rights reserved.

**Keywords:** Titanium dioxide; Nanocrystal; Anatase; Solvothermal synthesis; Characterization; Ultrahigh surface area

## 1. Introduction

Nanocrystalline titanium dioxide (TiO<sub>2</sub>) has emerged as an attractive multi-purpose material, its applications include in photovoltaic solar cells, gas sensors [1,2], catalytic oxidation of carbon monoxide and the photocatalytic decomposition of organic environmental contaminants [3–9]. Its widespread applications make the preparation extensively studied [10–32]. In recent years a wide variety of methods have been developed to produce nano-titania with properties tailored to different applications, such as aerosol pyrolysis, sol–gel technique, calcination of amorphous titania, and surfactant-based colloidal synthesis [10–17]. However, the products obtained in such syntheses are usually inadequate for the purposes of catalytic applications, which require nanocrystalline titania consisting mostly or entirely of fine-grained (<10 nm) anatase with extremely high specific surface area (>200 m<sup>2</sup> g<sup>-1</sup>) [18–21]. They either produce large primary particles (>20 nm) with low specific surface

areas surfactant molecules on particle surfaces prevents molecular species from accessing the active surface sites, thereby limiting the product's efficacy as a catalyst [10–17].

A surfactant-free hydrothermal technique (i.e., high-temperature, high-pressure) has been shown to be a suitable way for obtaining titania with small grain sizes, high specific surface areas, and high crystallinity [18,20–25]. In stead of aqueous system, ethanol, an organic solvent was chosen for our study. This solvothermal technique was recently introduced to synthesize some ceramic oxides [26–32], including nanocrystal TiO<sub>2</sub> powders [28–32]. These studies showed it had not only the advantages of hydrothermal synthesis, but also avoided contaminations from ion species dissolved in water, which improved the surface area and quality. It also makes it possible to probe the effects of the water:alkoxide molar ratio in same phase. Despite the advantages that solvothermal synthesis offers, however, it did not widely explore the relations between synthetic parameters and physical properties of the obtained particles, i.e., ratio of precursors to water in homogeneous phase (ethanol + water), and did not yields anatase with specific surface areas above 200 m<sup>2</sup> g<sup>-1</sup>.

<sup>\*</sup> Corresponding authors. Fax: +1 713 348 2578.  
E-mail addresses: [ypliu@rice.edu](mailto:ypliu@rice.edu) (Y. Liu), [colvin@rice.edu](mailto:colvin@rice.edu) (V.L. Colvin).

In the present work, a rapid solvothermal synthesis was developed to produce phase-pure, monodisperse anatase nanocrystals with small grain size and high specific surface area, correspondingly, the following processes were designed to maximize the performance of nanoscale titania in the many applications that rely on its surface chemistry: first inject a precursor solution directly into a pre-heated bomb reactor, which not only ensures rapid nucleation (and thus smaller particles) but also minimizes the amount of time and equipment required for each reaction. To further promote fine grain sizes and large surface areas, the reactions are performed at relatively low temperature (140–300 °C) using short reaction times so as to minimize grain growth via Ostwald ripening. Additionally, near-neutral conditions were adopted to encourage the exclusive formation of anatase; to guarantee a nearly neutral pH, an alkoxide precursor is used rather than  $\text{TiCl}_4$ , since the latter releases chloride ions into the reaction medium thus creating an acidic environment.

## 2. Experimental

### 2.1. Solvothermal synthesis

Solvothermal titania samples were prepared as follows: a known amount of ultrapure water (MilliQ, 18.2 M $\Omega$  cm) was dissolved in dry ethanol (90 mL, Pharmco Products) and heated with stirring inside a 450-mL, corrosion-resistant Monel autoclave (Parr Instruments, Model #4562), equipped with a temperature controller (Parr Instruments, Model #4843) and an automatic cooling loop. Once the reactor reached the desired reaction temperature, the precursor solution prepared in dry ethanol was transferred to a stainless steel pressure pipette and charged into the reactor. A momentary temperature decrease of 5–10 °C was observed upon injection of the ethoxide solution, but the target reaction temperature was restored within 1–2 min. The reaction mixture was stirred at constant temperature for 2 h and then quenched by plunging the bomb into a room-temperature water bath.

The cooled product mixture, consisted of white  $\text{TiO}_2$  powder suspended in ethanol, was transferred to a plastic beaker and agitated for 5–10 min in a sonication bath to break up aggregates, then the suspension was vacuum-filtered through a piece of Whatman 2 ashless filter paper in order to remove large aggregates from the product. The filtered  $\text{TiO}_2$  solid was isolated via a 10–30 min centrifugation at 4200 rpm, washed with either 190-proof ethanol (Pharmco Products) or MilliQ water, and dried either under vacuum or in an 80–90 °C oven.

### 2.2. Characterization

X-ray diffraction (XRD) spectra were taken using a Siemens Platform-Model General Area Detector Diffraction System (GADD) with a  $\text{CuK}\alpha$  source. Each spectrum was taken using a voltage of 50 kV, a current of 40 mA, and a total collection time of 10–60 min. Grain sizes were estimated according to the Debye–Scherrer formula with Warren’s correction for instrumental broadening [33].

Brunauer–Emmett–Teller (BET) surface areas were determined from  $\text{N}_2$  adsorption onto the titania powders using a Micromeritics ASAP 2010 apparatus. Samples were degassed for several hours at 150 °C (except the samples synthesized at 140 °C, which were degassed at room temperature) prior to the  $\text{N}_2$  adsorption analysis, which was carried out at liquid nitrogen temperature (–196 °C).

Transmission electron micrographs (TEM) were taken on a JEOL 2010 microscope. Each TEM sample was prepared by evaporating 1–5 drops of a sonicated ethanol suspension of titania onto a 300-mesh copper/carbon grid (Ted Pella, Inc.).

Raman spectra were taken on a Renishaw Ramascope apparatus using a He–Ne laser with an excitation wavelength of 633 nm. Collection times ranged from 10 to 60 s per spectrum.

Differential thermal analysis (DTA) was performed in air on a Thermal Advantage SDT 2960 apparatus using a temperature range of 25–600 °C and a heating rate of 20 °C  $\text{min}^{-1}$ .

## 3. Results and discussion

All the data in this paper are based on the ones that some of big aggregates were removed from the original products with filter paper although only around 1% amount were removed. The removed percentages in Table 1 actually include three parts in sum: big aggregates whose sizes are bigger than the hole sizes in the filter papers, some fine particles absorption to the filter papers and some particles lost in the collecting procedures.

### 3.1. Size, shape, and surface area

Fig. 1 shows the X-ray diffraction patterns of solvothermal titania prepared at temperatures between 140 and 300 °C. In all reactions for which  $T \geq 140$  °C the products were found to consist of phase-pure anatase, which is consistent with previous findings that anatase formation is favored at or near neutral pH under higher-temperature hydrothermal conditions [18,25]. It is interesting that even at temperatures as low as 140 °C, it is possible to obtain a crystalline product; the ability to process nanocrystalline anatase at such a low temperature is advantageous both because it requires less energy for manufacturing

Table 1  
Grain sizes, specific surface areas and removed amounts of the big aggregates for hydrothermal titania prepared with  $[\text{Ti}(\text{OEt})_4] = 0.02 \text{ mol L}^{-1}$  and  $r = 20$

$T$ (°C) or company	$d$ (nm)	$S_{\text{BET}}$ ( $\text{m}^2 \text{g}^{-1}$ )	$S_{\text{AExpected}}$ ( $\text{m}^2 \text{g}^{-1}$ )	$S_{\text{BET}}: S_{\text{AExpected}}$	Removed amount (%) <sup>a</sup>
140	5.35	250.6 ± 3.4	292.1	0.858	0.84
150	6.69	160.7 ± 0.7	233.6	0.688	1.01
200	7.72	–	202.4	–	0.85
220	8.85	127.7 ± 0.7	176.6	0.723	–
250	8.81	123.1 ± 0.9	177.4	0.694	1.03
275	16.70	–	93.6	–	0.89
300	16.17	60.8 ± 1.5	96.6	0.629	1.13
335	19.97	55.0 ± 0.9	78.2	0.703	0.93
Degussa P25	~21	50 ± 15	74.4	0.672	–
Altair TiNano	30–50	50 ± 10	31.3–52.1	0.960–1.597	–

<sup>a</sup> Removed amount (%): percentages of the big hard aggregates removed from its original samples.

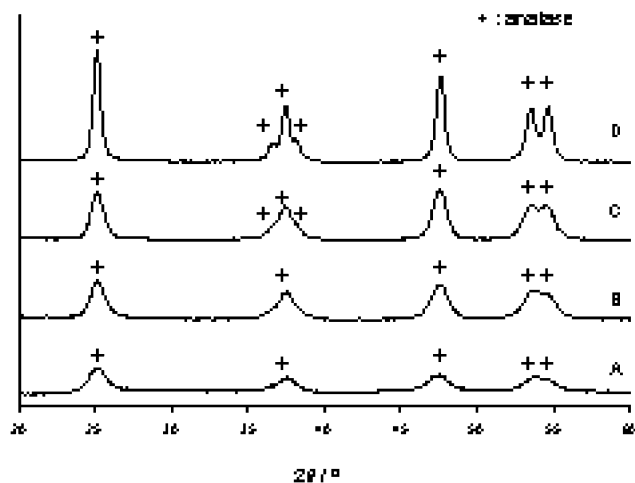


Fig. 1. X-ray diffraction spectra of solvothermal anatase produced at (A) 140 °C, (B) 150 °C, (C) 220 °C, and (D) 300 °C.

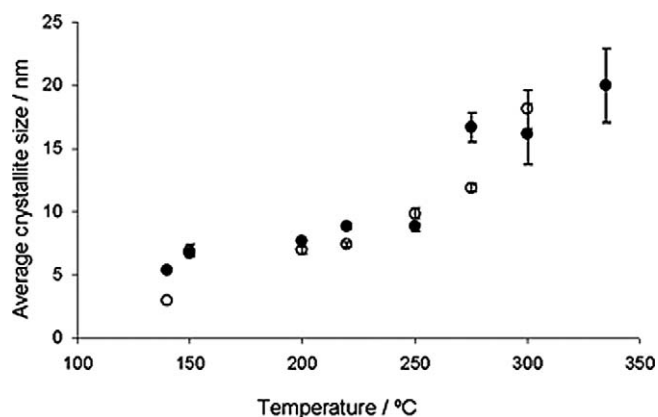


Fig. 2. Effect of reaction temperature on average grain size of solvothermally prepared anatase for hydrolysis ratios of  $r = 20$  (●) and  $r = 5$  (○). Samples were prepared using a  $\text{Ti}(\text{OEt})_4$  concentration of  $0.02 \text{ mol L}^{-1}$  and a total reaction time of 2 h.

and because lower temperatures tend to result in the formation of finer crystallites with larger specific surface areas.

The gradual narrowing of the XRD lines with increasing temperature reflects a corresponding increase in the average grain size [33], a trend that is quantitatively illustrated for two different hydrolysis ratios ( $r = 5$  and  $r = 20$ ) in Fig. 2. There appears to be very little difference between the size versus temperature plots for these two hydrolysis ratios; however, as will be discussed in the following section, it is possible that at intermediate hydrolysis ratios one could obtain even finer anatase crystallites than for reactions run with an excess of either water or alkoxide precursor.

A series of samples prepared with  $r = 20$  and  $[\text{Ti}(\text{OEt})_4] = 0.02 \text{ mol L}^{-1}$  at various temperatures was characterized by BET surface area measurements, the results of which were then compared to “expected” surface areas calculated from the XRD-derived grain sizes. The expected surface area of a sample was computed assuming perfectly spherical, unaggregated crystallites with a grain size determined by the XRD analysis and a mass density equal to that of bulk anatase, i.e.,  $\rho = 3.84 \text{ g cm}^{-3}$ . Table 1 shows the grain sizes ( $d$ ), experimental

surface areas ( $S_{\text{BET}}$ ), and expected surface areas ( $S_{\text{AExpected}}$ ) for the ( $r = 20$ ,  $[\text{Ti}(\text{OEt})_4] = 0.02 \text{ mol L}^{-1}$ ) samples prepared in this work as well as for two commercial nano- $\text{TiO}_2$  samples obtained from Degussa (P25) [34] and Altair (TiNano) [35].

Three features of these data are particularly noteworthy. First, by using a relatively low solvothermal reaction temperature ( $T = 140 \text{ °C}$ ), it is possible to prepare nanocrystalline anatase with a surface area of up to  $250 \text{ m}^2 \text{ g}^{-1}$ . Secondly, all of the samples prepared in this work possess larger surface areas than those reported for commercial titania samples; this is most likely due to the strategy of using a mild solvothermal treatment optimized to produce fine grains (and consequently larger surface areas). The aerosol methods by which Degussa and Altair manufacture their products cannot be easily controlled to provide grain sizes below 20 nm, and as a consequence their specific surface areas tend to be low ( $\sim 50 \text{ m}^2 \text{ g}^{-1}$ ) [34,35]. Finally, comparison of the experimental and expected surface areas for the solvothermally prepared powders indicates that our synthesis consistently yields a product with 63–86% of its ideal surface area. The significance of this last observation is that due to the absence of a surface stabilizing (peptizing) agent in the reaction medium, some of the primary particles in the product either contain defects that reduce their surface area or else form hard aggregates whose surfaces are unavailable for sorption. Because ultrafine ( $< 10 \text{ nm}$ ) crystals tend to have a very low number of defects, it is likely that the presence of hard aggregates in the product is responsible for the difference between the experimental and expected values for the specific surface areas of the solvothermal samples. Principally higher solvothermal temperature results in more hard aggregates, which could give an explanation to the highest BET surface area with the lowest reaction temperature of 140 °C, however, because some amount of big aggregates were removed from the samples, it cannot be given an trend of BET surface areas vs solvothermal reaction temperatures. Even so, a sufficient fraction of primary particles remain either unaggregated or loosely aggregated so that reasonably high surface areas are observed.

Transmission electron micrographs of the samples prepared with a hydrolysis ratio = 20 at 220 °C for 2 h show that corroborate both the temperature dependence of grain size and the interpretation of the BET data; in addition to the obvious increase in average crystallite size from the 150 °C (Fig. 3a) sample to the 300 °C sample (Fig. 3b), it is clear from these images that in both samples some individual crystallites form hard aggregates, while other crystallites form relatively loose aggregates.

The most striking revelation in the TEM images, however, is that temperature has a pronounced effect on particle morphology and distribution. Specifically, the particle sizes and shapes appear to shift from a unimodal distribution of roughly spherical crystals at 150 °C to a bimodal distribution, consisting mostly of 10–15 nm spheres with a smaller number of  $\sim 40 \text{ nm}$  cubes, at 300 °C. The appearance of larger particles with new morphology at the latter temperature suggests that higher reaction temperatures are conducive to grain growth via a dissolution–reprecipitation mechanism (i.e., Ostwald ripen-

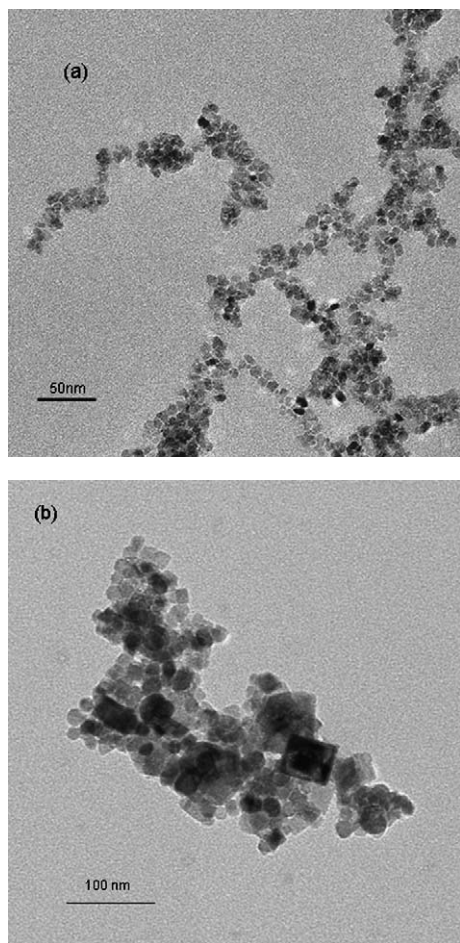
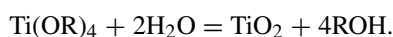


Fig. 3. TEM images of solvothermal anatase prepared at (a) 150 °C and (b) 300 °C.

ing) in which larger particles grow at the expense of smaller ones. The relatively small fraction of large cubes present in the 300 °C product is most likely due to the solvothermal reaction time (2 h), which is considerably shorter than the treatment times (1 or more days) used in other studies (e.g., Wang and Ying [18]). An increase in aging time would presumably result in more extensive Ostwald ripening and consequently a greater number of large cubic nanocrystals.

Fig. 4 shows the effect of initial  $\text{Ti}(\text{OEt})_4$  concentration on anatase grain size for a series of samples prepared with a hydrolysis ratio of  $r = 20$  at 220 °C. Based on a reaction formula of  $[\text{Ti}(\text{OR})_4]$  hydrolysis to obtain  $\text{TiO}_2$ ,



A ratio of water to  $\text{Ti}(\text{OR})_4$  for completely hydrolysis of  $\text{Ti}(\text{OR})_4$  should be 2. Here  $r = 20$  was chosen to ensure its complete hydrolysis. Clearly an increase in the precursor concentration results in the formation of larger crystallites, which is to be expected since more material is available for growth onto each crystal after nucleation. However, the grain sizes start to increase more slowly once  $[\text{Ti}(\text{OEt})_4]$  exceeds 0.04–0.05  $\text{mol L}^{-1}$ , which suggests that at higher supersaturations the process of nucleation competes with grain growth to a greater extent than at low supersaturations.

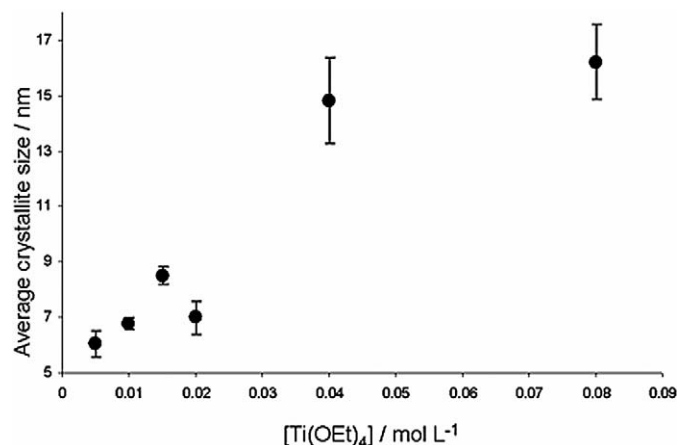


Fig. 4. Effect of precursor concentration on average grain size of solvothermally prepared anatase. Samples were prepared at 220 °C using a hydrolysis ratio of  $r = 20$  and a total reaction time of 2 h.

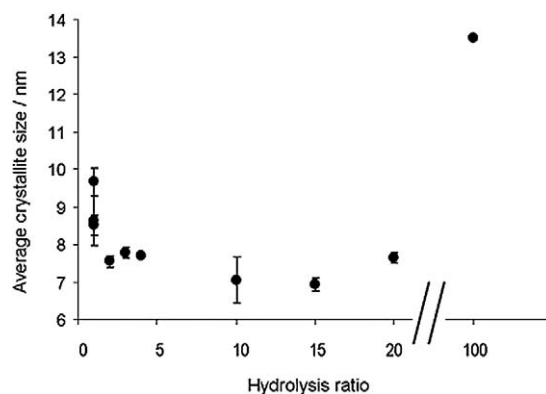


Fig. 5. Effect of hydrolysis ratio on average grain size of solvothermally prepared anatase. Samples were prepared at 220 °C using a  $\text{Ti}(\text{OEt})_4$  concentration of 0.02  $\text{mol L}^{-1}$  and a total reaction time of 2 h.

The effect of the hydrolysis ratio on grain size was studied for a group of reactions conducted at 220 °C using  $[\text{Ti}(\text{OEt})_4] = 0.02 \text{ mol L}^{-1}$  and a total reaction time of 2 h. Fig. 5 shows the results of varying the hydrolysis ratio between  $r = 1$  and  $r = 100$  under these conditions. The plot of crystallite size as a function of hydrolysis ratio exhibits a minimum between  $r$  values of 5 and 15. At low  $r$  values, i.e.,  $1 \leq r \leq 10$ , the results of the present work are in qualitative agreement with previous reports that an increase in the hydrolysis ratio favors the formation of finer crystallites [24,25]. However, above a hydrolysis ratio of  $r \cong 15$ , the grain size data obtained here begin to follow an upward trend as  $r$  further increases.

It is likely that the data shown in Fig. 5 reflect a competition between two or more factors. One possible explanation for the observation of minimal sizes at intermediate  $r$  values is that an increase in  $r$  results in both (a) an increase in the anatase nucleation rate, which favors finer crystallites, and (b) enhanced hydrogen bonding among the nuclei once they form, a process that favors grain growth. The former effect could arise from a faster, more complete hydrolysis of the precursor, which would encourage the formation of a large number of anatase nuclei in a short amount of time [18]. On the other hand, one can also expect more extensive hydrogen bonding among anatase nu-

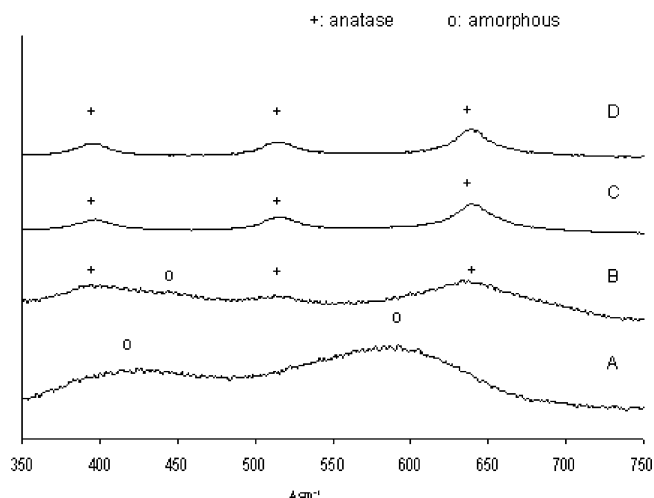


Fig. 6. Evolution of  $\text{TiO}_2$  Raman spectra with reaction temperature. Samples were prepared at (A) 25 °C, (B) 140 °C, (C) 150 °C, and (D) 220 °C using a hydrolysis ratio of  $r = 20$ , a  $\text{Ti}(\text{OEt})_4$  concentration of  $0.02 \text{ mol L}^{-1}$ , and a total reaction time of 2 h.

clei at high  $r$  values than at low  $r$  values, which would tend to promote the agglomeration of those nuclei to eventually form coarser primary particles [36]. If anatase nucleation and hydrogen bonding are indeed competitive processes in the present solvothermal synthesis, it follows that the smallest crystallites would be obtained at  $r$  values for which accelerated nucleation is the dominant effect. Based on the results in Fig. 5, the enhanced nucleation rate appears to dominate over hydrogen bond-facilitated growth at intermediate  $r$  values ( $5 \leq r \leq 15$ ), whereas the reverse is true at very low ( $r < 5$ ) or very high ( $r > 15$ ) hydrolysis ratios.

### 3.2. Amorphous content and thermal stability

Both Raman spectroscopy and differential thermal analysis (DTA) were used to assess the amorphous content of hydrothermal titania samples prepared at different temperatures. For these analyses, a control sample consisting entirely of amorphous  $\text{TiO}_2$  was prepared by hydrolyzing  $\text{Ti}(\text{OEt})_4$  in dry ethanol solvent inside the bomb at 25 °C. Fig. 6 shows the evolution of the samples' Raman spectra with an increase in reaction temperature. The results indicate that for temperatures below 150 °C there is an obvious amount of amorphous material as the temperature is lowered further, until a completely amorphous solid is observed for a room-temperature reaction.

Differential thermal analysis (DTA) of the hydrothermal samples corroborates the Raman spectroscopic evidence of increased crystallinity at higher reaction temperatures. Fig. 7a, which shows the DTA profiles of samples prepared at or below 220 °C, illustrates the gradual disappearance of amorphous material as the reaction temperature is increased. Samples containing amorphous titania often exhibit an exothermic DTA peak between 350 and 450 °C, indicating crystallization of amorphous material to the anatase phase [36]. In the control sample prepared at 25 °C (curve A), crystallization is observed at approximately 425 °C, while the samples prepared at 100 and 140 °C (curves B and C) exhibit crystallization peaks at 350 and

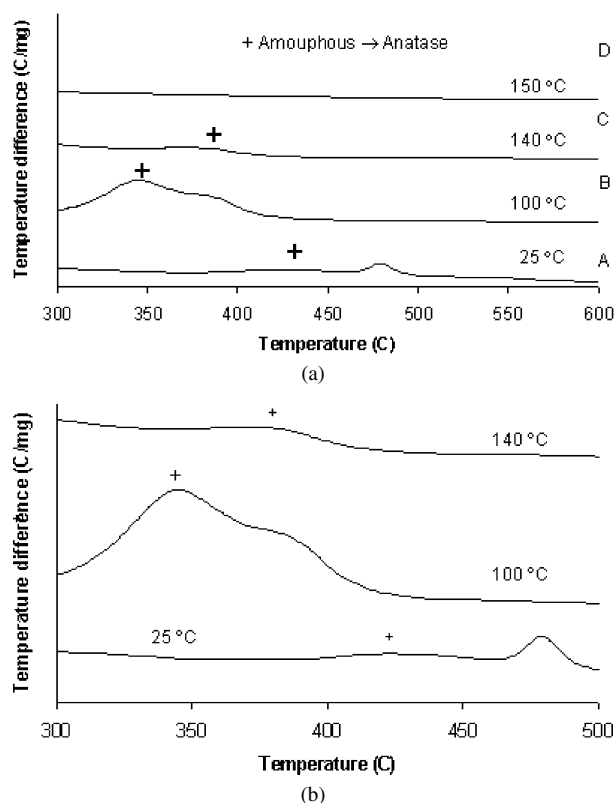


Fig. 7. (a) Evolution of differential thermal analysis (DTA) spectra with reaction temperature. Samples were prepared at (A) 25 °C, (B) 100 °C, (C) 140 °C, (D) 150 °C. (b) Influence of reaction temperature on DTA crystallization temperatures.

375 °C, respectively. Once the reaction temperature is raised to 150 °C (curve D), the exothermic amorphous  $\rightarrow$  anatase transition peak disappeared. However, XRD patterns in Fig. 1 show an increasing trend of intensity of diffraction peaks with increasing solvothermal reaction temperatures from 140 °C (A) to 300 °C (D), evidencing that the completely crystallization needs a relatively high temperature, at least  $T \geq 300$  °C.

The decrease in crystallization temperature from the 25 °C control sample to the 100 °C sample indicates that some crystalline material is forming even at 100 °C; as has been reported by several authors, the presence of a small amount of crystalline material in an otherwise amorphous sample reduces the temperature at which the amorphous material crystallizes [37–39]. On the other hand, increasing the hydrothermal reaction temperature from 100 to 140 °C causes a slight increase in crystallization temperature (from 350 to 375 °C). It may be that in samples processed at higher temperatures, the amorphous materials are denser than those prepared at lower temperatures and therefore require greater thermal energy to dissolve and subsequently crystallize.

Fig. 8 shows XRD spectra for the heat-treated samples in the present work; these spectra confirm that the low-crystallinity titania samples prepared below 140 °C contain both anatase and rutile after heat treatment, while the high-crystallinity samples prepared at or above 140 °C consist entirely of anatase even after heating to 600 °C and are therefore thermally resistant to conversion to rutile. Additionally, the heat-treated 100 °C sam-

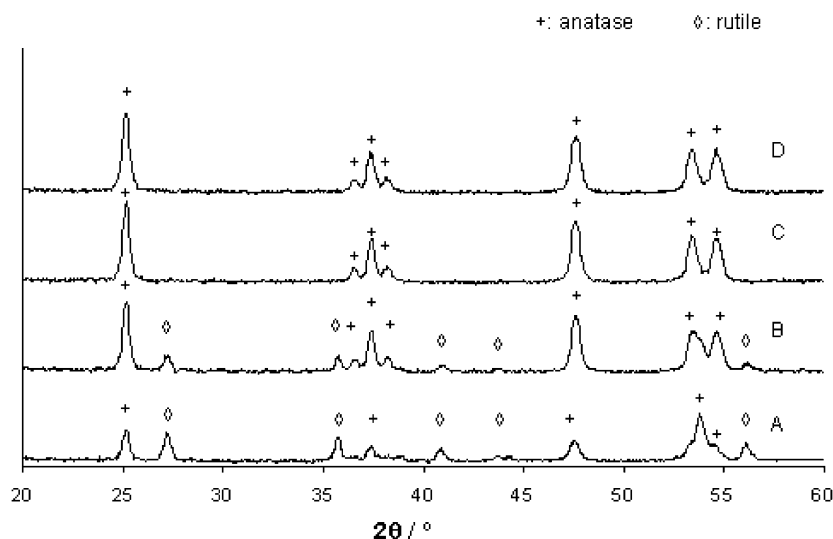


Fig. 8. XRD spectra of hydrothermal  $\text{TiO}_2$  samples after heating to  $600\text{ }^\circ\text{C}$  in a differential thermal analyzer. Original preparation temperatures were (A)  $25\text{ }^\circ\text{C}$ , (B)  $100\text{ }^\circ\text{C}$ , (C)  $140\text{ }^\circ\text{C}$ , and (D)  $150\text{ }^\circ\text{C}$ .

ple contains a smaller fraction of rutile than the heat-treated  $25\text{ }^\circ\text{C}$  control sample, suggesting that the slightly higher crystallinity of the as-prepared  $100\text{ }^\circ\text{C}$  sample renders it more thermally stable against the anatase  $\rightarrow$  rutile transformation. In this case, then, a higher degree of crystallinity correlates with increased thermal stability.

#### 4. Conclusions

A mild solvothermal synthesis ( $<200\text{ }^\circ\text{C}$ , 2 h) has been used to prepare ultrafine, phase-pure nanocrystalline anatase with specific surface area up to 5 times that of commercially available nano-titania. The physical properties of the hydrothermal product can be fine-tuned by adjusting the temperature, precursor concentration, and hydrolysis ratio of the reaction. It is possible to obtain a very fine-grained crystalline product with high thermal stability and ultrahigh surface area using relatively low reaction temperatures  $140\text{--}150\text{ }^\circ\text{C}$ . The results of this work suggest that the grain size might be reduced even further by optimizing the concentration of alkoxide precursor and the water:alkoxide ratio.

#### Acknowledgments

We thank Dr. Andreas Lüttge and his research group for the use of their Micromeritics ASAP 2010 BET apparatus, the Degussa Corporation for supplying us with P25, Dr. Mason Tomson's research group for providing samples of TiNano (Altair), the Dupont Corporation for its support, and the National Science Foundation and Rice University's Center for Biological and Environmental Nanotechnology (Grant EEC-0118007) for funding this research.

#### References

- [1] C.J. Barbe, F. Arendse, P. Comte, M. Jirousek, F. Lenzmann, V. Shklover, M. Gratzel, *J. Am. Ceram. Soc.* 80 (1997) 3157–3171.

- [2] M. Ferroni, V. Guidi, G. Martinelli, G. Faglia, P. Nelli, G. Sberveglieri, *Nanostruct. Mater.* 7 (1996) 709–718.
- [3] Y.D. Kim, M. Fischer, G. Gantefor, *Chem. Phys. Lett.* 377 (2003) 170–176.
- [4] L. Rideh, A. Wehrer, D. Ronze, A. Zoulalian, *Ind. Eng. Chem. Res.* 36 (1997) 4712–4718.
- [5] B. Schumacher, V. Plzak, M. Kinne, R.J. Behm, *Catal. Lett.* 89 (2003) 109–114.
- [6] A.G. Agrios, K.A. Gray, E. Weitz, *Langmuir* 19 (2003) 1402–1409.
- [7] Z. Ding, G.Q. Lu, P.F. Greenfield, *J. Phys. Chem. B* 104 (2000) 4815–4820.
- [8] M.K.S. Mak, S.T. Hung, *Toxicol. Environ. Chem.* 36 (1992) 155–168.
- [9] S.-J. Tsai, S. Cheng, *Catal. Today* 33 (1997) 227–237.
- [10] P.P. Ahonen, E.I. Kauppinen, J.C. Joubert, J.L. Deschanvres, G. Van Tendeloo, *J. Mater. Res.* 14 (1999) 3938–3948.
- [11] Y. Li, T. Ishigaki, *Chem. Mater.* 13 (2001) 1577–1584.
- [12] X.-Z. Ding, X.-H. Liu, *Mater. Sci. Eng. A* 224 (1997) 210–215.
- [13] H. Zhang, M. Finnegan, J.F. Banfield, *Nano Lett.* 1 (2001) 81–85.
- [14] J. Yang, S. Mei, J.M.F. Ferreira, *J. Am. Ceram. Soc.* 84 (2001) 1696–1702.
- [15] A. Chemseddine, T. Moritz, *Eur. J. Inorg. Chem.* (2) (1999) 235–245.
- [16] H. Yin, Y. Wada, T. Kitamura, S. Kambe, S. Murasawa, H. Mori, T. Sakata, S. Yanagida, *J. Mater. Chem.* 11 (2001) 1694–1703.
- [17] S.Y. Chae, M.K. Park, S.K. Lee, T.Y. Kim, S.K. Kim, W.I. Lee, *Chem. Mater.* 15 (2003) 3326–3331.
- [18] C.-C. Wang, J.Y. Ying, *Chem. Mater.* 11 (1999) 3113–3120.
- [19] C.-C. Wang, Z. Zhang, J.Y. Ying, *Nanostruct. Mater.* 9 (1997) 583–586.
- [20] H. Hayashi, K. Torii, *J. Mater. Chem.* 12 (2002) 3671–3676; H. Kominami, T. Matsuura, K. Iwai, B. Ohtani, S. Nishimoto, Y. Kera, *Chem. Lett.* 1995 (1995) 693–694.
- [21] Y. Oguri, R.E. Riman, H.K. Bowen, *J. Mater. Sci.* 23 (1988) 2897–2904.
- [22] A.J. Maira, K.L. Yeung, C.Y. Lee, P.L. Yue, C.K. Chan, *J. Catal.* 192 (2000) 185–196.
- [23] Z. Ma, Y. Yue, X. Deng, Z. Gao, *J. Mol. Catal. A Chem.* 178 (2002) 97–104.
- [24] J. Ovenstone, K. Yanagisawa, *Chem. Mater.* 11 (1999) 2770–2774.
- [25] K. Yanagisawa, J. Ovenstone, *J. Phys. Chem. B* 103 (1999) 7781–7787.
- [26] Y.-W. Zhang, R. Si, C.-S. Liao, C.-H. Yan, C.-X. Xiao, Y. Hou, *J. Phys. Chem. B* 107 (2003) 10159–10167.
- [27] H. Kominami, K. Matsuo, Y. Kera, *J. Am. Ceram. Soc.* 79 (1996) 2506–2508.
- [28] M. Kang, *J. Mol. Catal. A Chem.* 197 (2003) 173–183.
- [29] H. Kominami, Y. Takada, H. Yamagiwa, Y. Kera, *J. Mater. Sci. Lett.* 15 (1996) 197–200.
- [30] C. Wang, Z.-X. Deng, Y. Li, *Inorg. Chem.* 40 (2001) 5210–5214.

- [31] H. Kominami, J. Kato, S. Murakami, Y. Kera, M. Inoue, T. Inui, B. Ohtani, *J. Mol. Catal. A Chem.* 144 (1999) 165–171.
- [32] H. Kominami, M. Kohno, Y. Takada, M. Inoue, T. Inui, Y. Kera, *Ind. Eng. Chem. Res.* 38 (1999) 3925–3931.
- [33] H.P. Klug, L.E. Alexander, *X-Ray Diffraction Methods for Polycrystalline and Amorphous Materials*, Wiley & Sons, New York, 1974.
- [34] <http://www.altairnano.com>, 2003.
- [35] <http://www.degussa.de/en/products.html>, 2003.
- [36] J.P. Hsu, A. Nacu, *Langmuir* 19 (2003) 4448–4454.
- [37] C. Liu, S. Komarneni, R. Roy, *J. Am. Ceram. Soc.* 77 (1994) 3105–3112.
- [38] C. Liu, S. Komarneni, R. Roy, *J. Am. Ceram. Soc.* 78 (1995) 2521–2526.
- [39] P. Ravindranathan, S. Komarneni, R. Roy, *J. Am. Ceram. Soc.* 73 (1990) 1024–1025.